Čerenkov radiation from a finite-length path in a gas

John R. Neighbours, Fred R. Buskirk, and A. Saglam
Physics Department, Naval Postgraduate School, Monterey, California 93940
(Received 5 August 1983)

Measurements of microwave Čerenkov radiation in air show that the Čerenkov cone angle is broadened as predicted in earlier work. Extension of previous theory shows that for small Čerenkov angles, the broadening is asymmetric, giving an increase in the effective cone angle to a value in agreement with the experimental results. The shift in the radiation peak can be understood as a diffraction effect arising from the linearly varying phase of the radiation along the beam interaction length.

INTRODUCTION

Čerenkov radiation has been well studied,[1-3] principally for radiation emitted in the optical region. Recent interest in Čerenkov radiation within a different frequency range[4] has been initiated by the possible availability of intense relativistic beams. References 1–3 contain extensive listings of the older literature and Ref. 4 lists the relevant later work.

In our previous work,[4,5] Čerenkov radiation was considered for periodic bunches of electrons such as would be emitted by a typical traveling-wave electron linear accelerator (linac). Even in air, electrons from a 100-MeV linac exceed the velocity of light in the medium, and radiation is expected to be emitted at a small angle of less than 2°. The radiation intensity was calculated in detail for microwave frequencies and some of the results follow.

(a) For bunches periodic in time with frequency ν_0, radiation is emitted at ν_0 and harmonics thereof, in contrast with the continuous frequency distribution observed for a single charge.

(b) If each bunch has a spatial distribution described by a charge density $\rho_0'(\vec{r})$, the radiated intensity is modified by the Fourier transform of this charge distribution.

(c) At low frequencies such that the wavelength of the emitted radiation is of the order of the bunch size, the electrons in the bunch radiate coherently. This leads to large enhancement factors for typical linac bunches consisting of 10^8 electrons, and in fact allows the radiation to be significant at microwave frequencies. Destructive interference, described by the Fourier transform of the charge density, decreases intensities with increasing frequency, until incoherent radiation takes over when the wavelength of the radiation is much less than the electron spacing.

(d) If the emission region has finite length, which may be realized by passing the electron beam through a gas cell, the radiation propagation direction is not confined to a sharp Čerenkov angle $\theta_{\check{C}}$, where $\cos\theta_{\check{C}}$ is defined to be c/v, but is spread over a range of emission angles. This spreading effect depends only on the path length in the gas and does not depend on the electron bunch structure or periodicity of the bunches.

(e) In addition, the observation of microwave Čerenkov radiation was noted but not reported in any detail.

In this paper, some experimental results are reported which show that the peak in the microwave Čerenkov radiation occurs at angles greater than the ordinary Čerenkov angle. These results are understood by an extension of the results of Ref. 4.

EXPERIMENTAL

Microwave Čerenkov radiation has been investigated in several different arrangements. In all these experiments, except as noted, the detector unit was a short ($\sim$15 cm) length of waveguide with a horn attached at the receiving end and a crystal diode mounted on the opposite end. The source of high-speed electrons was the Naval Postgraduate School 100 MeV linac operating at S band with a current of approximately 20 mA.

In our first observations of microwave Čerenkov radiation, an X-band detector unit was mounted on a motorized track so as to be movable along a line perpendicular to the electron beam. With the beam passing through air, X-band radiation was observed and the radiation angle was seen to be different from the Čerenkov angle. In the second series of experiments, which confirmed that the

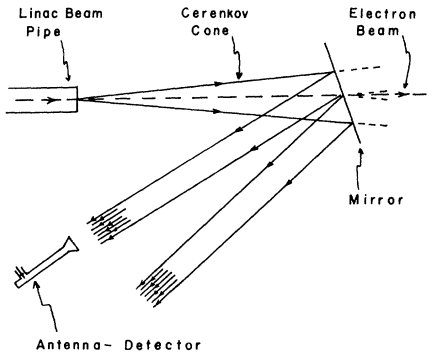

FIG. 1. Schematic experimental arrangement. Electrons pass from the accelerator into air and generate Čerenkov radiation which is reflected by the metal mirror. A hollow cone of radiation is formed as shown since the radiation is generated only in the region between the beam pipe and the mirror. The highly relativistic electrons pass through the mirror. The antenna-detector assembly can be translated on a track (not shown). In this figure, no diffraction effects are shown.

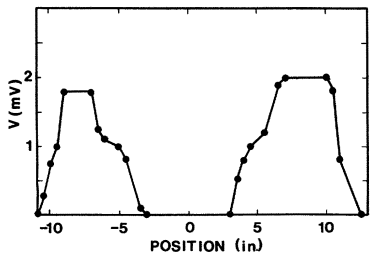

FIG. 2. X-band (7—12 GHz) signal amplitude V as a position of detector. $L_1=89$ cm and $L_2=99$ cm.

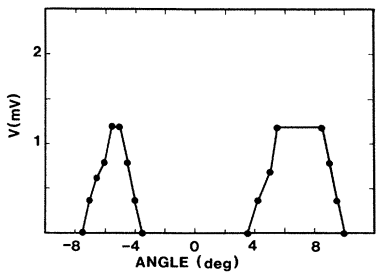

FIG. 3. X-band (7—12 GHz) signal amplitude V as a function of mirror rotation angle. $L_1=89$ cm and $L_2=99$ cm.

microwave radiation occurred at multiples of the linac frequency, a fixed horn mounted to intercept the peak radiation was connected via long lengths of X-band waveguide to a spectrum analyzer located in the control room. These observations were mentioned in earlier work, but have otherwise gone unreported.

In the third series of measurements, as shown schematically in Fig. 1, the electron beam emerged from the end window of the accelerator and passed through a flat metal sheet a distance L_1 downstream, oriented at an angle ϕ from the normal to the beam. The metal sheet defined a finite length of gas radiator and reflected the Čerenkov cone of radiation toward the accelerator, but rotated by an angle 2ϕ from the beam line. A microwave X-band antenna and crystal detector with response from 7 to above 12 GHz was mounted on a track so that the assembly could be moved across the reflected Čerenkov cone as a probe. The track was located a distance L_2 from the mirror and was adjusted to be perpendicular to the reflection of the beam line so that motion of the detector along the track would intercept both sides of the Čerenkov cone. Figure 2 shows the X-band detector voltage as a function of position for a setup where the distance from the electron source to the mirror (L_1) was 89 cm and the distance from the mirror to the track (L_2) was 99 cm. Similar results were observed in the K band and in both bands using different lengths L_1 and L_2.

Since radiation occurs all along the electron beam, it is difficult to determine the radiation angle from measurements made relatively close to the beam. If the center of the beam path (i.e., $L_1/2$) is assumed to be the origin for the centers of the peaks displayed in Fig. 2, the radiation angle is determined from

$$\tan\theta=\frac{x}{L_1+2L_2}\ , \tag{1}$$

where x is the distance between peak centers.

Equation (1) gives a value of $\theta=8.2°$ for the results shown in Fig. 2, which is far in excess of the Čerenkov angle as calculated from $\cos\theta_{\check{C}}=c/v$. Other criteria, such as the outside of the radiation pattern originating directly at the electron source, may be used to analyze the data of Fig. 2, but the resulting angles are always much larger than $\theta_{\check{C}}$.

A fourth series of experiments used the arrangement of the third series (Fig. 1), but the detector unit was fixed and the mirror rotated to scan the Čerenkov radiation past the detector. Figure 3 shows the X-band detector voltage as a function of mirror-rotation angle α for lengths $L_1=89$ cm and $L_2=99$ cm. Again, since the detector unit was at a finite distance L_2 from the radiating length L_1, it is somewhat difficult to define the radiation angle. For small angles one can show that

$$\theta=\frac{2L_2}{L_1+2L_2}\alpha\ , \tag{2}$$

which gives an angle of 8.3° for the peak in Fig. 3. Similar results were obtained for the K band and for other lengths.

Table I shows the angle of the radiation peaks for the different geometries and bands. Although the experiment and its analysis are crude in many respects, two points are clear.

(a) The observed peak in the microwave Čerenkov radiation occurs at an angle much larger than that expected from application of the ordinary Čerenkov formula.

(b) The observed peak occurs at a larger angle for X-band radiation than for K-band radiation.

RESULTS OF PREVIOUS CALCULATIONS

In this paper, as in previous ones, the velocity of light and wave vector in the medium are represented by c and

TABLE I. Summary of results of microwave-Čerenkov-radiation experiments.

Experiment	L_1 (cm)	L_2 (cm)	α (degrees)	Peak angle X band	Peak angle K band
Traveling detector	89	99		8.2°	5.9°
	66	89		9.1°	7.0°
Rotating mirror	89	99	12	8.3°	6.0°
	109	114	11	7.4°	5.4°
Average				8.25°	6.08°

k, respectively. The power radiated from periodic bunches of electrons traveling at a velocity v greater than the speed of light c in a medium has been given in Eqs. (25)–(27) of Ref. 4. For convenience they are written below using slightly different terminology. The power radiated per unit solid angle $dP/d\Omega$ is

$$\frac{dP}{d\Omega}=r^2\frac{1}{T}\int_0^T \hat{n}\cdot\vec{S}\,dt=\frac{2r^2}{\mu}\sum_0^\infty \frac{\omega^2}{C}\,|\,\hat{n}\times\tilde{\vec{A}}(\vec{r},\omega)\,|^2$$

$$=\sum_0^\infty W(\nu,\hat{n})\,, \tag{3}$$

where $W(\nu,\hat{n})$, the power per unit solid angle radiated at the frequency $\nu=ck/2\pi$, is

$$W(\nu,\hat{n})=\frac{\mu c\nu_0^2 q^2}{8\pi^2}\,|\,F(\vec{k})\,|^2[(kL)^2\sin^2\theta I^2(u)]\,. \tag{4}$$

The parameters describing the radiation are

$$u=\frac{kL}{2}(\cos\theta_{\check{C}}-\cos\theta)\,,$$

$$I(u)=\frac{\sin u}{u}\,,$$

$$\vec{k}=\left[n_x\frac{\omega}{c},n_y\frac{\omega}{c},\frac{\omega}{v}\right], \tag{5}$$

$$\tilde{\rho}_0'(\vec{k})=\int_{-\infty}^{\infty}\int_{-\infty}^{\infty}\int_{-\infty}^{\infty}dx\,dy\,dz\exp[-i\vec{k}\cdot\vec{r}]\rho_0'(\vec{r})$$

$$=qF(\vec{k})\,,$$

where n_x,n_y,n_z are components of the unit vector $\hat{n}$ in the emission direction, ν is the frequency of the emitted radiation, L $(=2Z')$ is the length of the gas cell, and the usual Čerenkov angle $\theta_{\check{C}}$ is given by $\cos\theta_{\check{C}}=c/v$. The total charge of one bunch is q, corresponding to a charge distribution $\rho_0'(\vec{r})$ with Fourier transform $\tilde{\rho}_0'(\vec{k})$, and $F(\vec{k})$ is defined as a dimensionless form factor. The bunch frequency ν_0 is equal to the electron velocity divided by the electron bunch spacing Z $(\nu_0=v/Z)$, and ν, the frequency of the emitted radiation, will be a harmonic of ν_0.

The results above are general ones for the emission of radiation from periodic bunches of electrons. In (4), the quantity enclosed in square brackets is a dimensionless radiation function. The factor $L^2I^2(u)$ is identical to the result obtained for the calculation of elementary Fraunhofer diffraction from a slit across which the phase varies linearly, such as plane waves striking the slit at an angle to the normal. However, in (4) the diffraction angle is not the usual one measured from the normal to the radiating line source. Here it is more convenient to measure the diffraction angle θ from the electron beam line so that it is the complement of the usual one. The $\sin^2\theta$ factor arises from cross products used in calculating the Poynting vector. It is just the angular factor in the usual expression for the power radiated from a dipole oriented along the electron beam. Thus the expression (4) for W can be interpreted as the interference of dipole radiators whose phase varies linearly with position along the beam line.

In the expression [Eq. (4)], for the radiated power per unit solid angle the factor $I^2(u)$ is strongly peaked at $u=0$. (When $u=0$, the radiation angle is equal to the Čerenkov angle $\theta_{\check{C}}$.) In an earlier paper, W was integrated over solid angle to obtain the total radiated power, assuming that I was so strongly peaked that the other functions in the integrand, namely $\sin^2\theta$ and $\tilde{\rho}_0'(\vec{k})$, could be evaluated at $\theta_{\check{C}}$ and taken outside the integral. Figure 1 of the previous paper shows the behavior of I^2 as a function of θ, and there is defined a width $\Gamma=\Delta G=\pi/2Z'$. If, in fact, the $\sin\theta$ and $\tilde{\rho}_0'(\vec{k})$ factors are slowly changing through the peak in I, the radiation is concentrated near the Čerenkov angle $\theta_{\check{C}}$ and the total radiated power is given by Eq. (32) of the earlier paper, which is

$$P_\omega=\frac{\mu}{4\pi}v\sin^2\theta_{\check{C}}\,|\,\tilde{\rho}_0'(\vec{k})\,|^2N\,, \tag{6}$$

where N is the number of pulses in the interacting region.

When $I(u)$ is not so strongly peaked, then the variation of the terms $\sin^2\theta$ and $\tilde{\rho}_0'(\vec{k})$ in the expression for W must be considered. In general, both factors should effect the position and height of the maximum in W, with the $\sin^2\theta$ term being predominant at smaller angles.

To continue, it is convenient to obtain a more specialized expression for W, and to that end, to introduce the harmonic number $j=\nu/\nu_0$ and to assume a particular charge density distribution

$$\tilde{\rho}_0'(\vec{k})=q\exp\left[-\frac{b^2k^2}{4}\cos^2\theta-\frac{a^2k^2}{4}\sin^2\theta\right] \tag{7}$$

which corresponds to a spatial charge distribution defined by a Gaussian

$$\rho_0'(\vec{r})=C_1\exp\left[-\frac{x^2}{a^2}-\frac{y^2}{a^2}-\frac{z^2}{b^2}\right], \tag{8}$$

where C_1 is a normalization constant related to the total charge per bunch and a,b are size parameters for the radial and longitudinal dimensions of the bunch. For a narrow electron beam, a, the parameter describing the radial dimension of the bunch, can be neglected so that W can be written

$$W(\nu,\theta)=W_j(\theta)=QD_j(\theta)\,, \tag{9}$$

where the radiation function is

$$D_j(\theta)=\frac{j^2}{4}L^2\sin^2\theta\left[\frac{\sin u}{u}\right]^2\exp\left[-\frac{k_z^2b^2}{2}\right], \tag{10}$$

the constant Q is

$$Q=\frac{2\mu\nu_0^4q^2}{c}\,,$$

the diffraction variable is

$$u=\frac{kL}{2}(\cos\theta_{\check{C}}-\cos\theta)\,, \tag{11}$$

and k_z has been written for $k\cos\theta$.

Although the function $D_j(\theta)$ is not dimensionless (it has dimensions of length squared), it is convenient to use in the case where the cell length is fixed and radiation

occurs at harmonics of the fundamental frequency ν_0. It is worthwhile noting that the frequency of radiation enters into W not only as the jth harmonic but also through the wave vector k (in the medium) in the expression (11) for the diffraction variable.

MICROWAVE ČERENKOV RADIATION IN A GAS

Equation (4) is generally applicable for electron bunches moving in a dielectric at velocities greater than the speed of light and (9) is the special case for a fine Gaussian beam. The central result of this work is a detailed discussion of the results predicted by (9) for the radiated microwave power in a gaseous medium and their comparison with experiment.

The Čerenkov angle defined by $\cos\theta_{\check{C}}=c/v=1/n\beta$ is small for most gases because n, the index of refraction of the gas, is very close to one. Consequently the dependence of $\theta_{\check{C}}$ on the electron velocity is very slight since β must also be close to one in order to attain the Čerenkov condition. Thus even for extremely relativistic electrons traveling in a typical gas, $\theta_{\check{C}}$ is always small (less than 2°).

Inspection of (11) shows that $u=0$ when $\theta=\theta_{\check{C}}$, a condition which leads to a maximum in the diffraction function $I^2(u)=(\sin u/u)^2$. Further inspection shows that if kL is large, then u will be large at angles significantly different from $\theta_{\check{C}}$, leading to $I^2(u)$ varying rapidly as a function of θ. In the limit as $kL\to\infty$ the diffraction function behaves like a δ function, having only the central maximum at $u=0$. This limiting behavior occurs regardless of the particular value of $\theta_{\check{C}}$ with an expression for the total radiated power given by (6).

For finite kL, the radiation is emitted with a finite range of angles centered about an angle other than $\theta_{\check{C}}$. Although the proper variable for discussing the radiation pattern is the product kL as seen in (4), it is more convenient to discuss predicted results in terms of the variation with either k alone or L alone.

In the range of θ in the vicinity of $\theta_{\check{C}}$, the $\sin^2\theta$ factor in (10) changes very rapidly although $\tilde{\rho}'_0(\vec{k})$ changes very little. Consequently the radiation then becomes not only smeared about the Čerenkov angle, but the angles greater than $\theta_{\check{C}}$ account for more radiated power than the angles between 0 and $\theta_{\check{C}}$. The result is that not only is the radiation distributed in the angle about $\theta_{\check{C}}$, but the distribution is distorted so that the peak of intensity may occur at several times $\theta_{\check{C}}$.

To calculate and plot expected results, a set of parameters were chosen close to those available in an experiment. A dielectric constant of $\epsilon=1.000\,536$ was assumed for air, giving an index of refraction of $n=1.000\,268$. The electron parameters were assumed to be those for a 100-MeV linac: fundamental frequency $\nu_0=2.85$ GHz and a Gaussian bunch parameter of $b=0.24$ cm. The gas-cell length was assumed to be 90 cm—also experimentally attainable.

Under these conditions, the calculated behavior of $D_j(\theta)$ is shown in Fig. 4 for the two haramonics $j=3$ and 5. The expected Čerenkov angle is calculated to be $\theta_{\check{C}}=1.29°$ and the striking result is how far the maxima in the high-intensity (first) lobes are displaced from $\theta_{\check{C}}$.

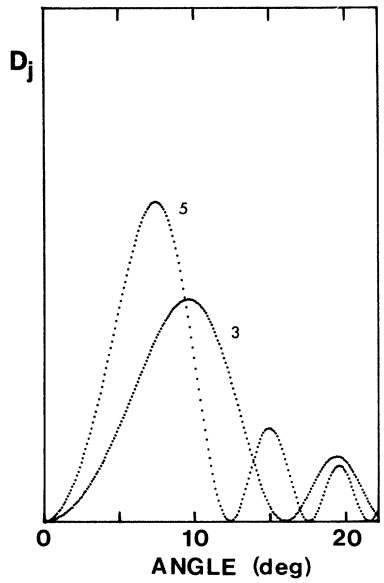

FIG. 4. Radiation function D_j for the harmonics $j=3$ and 5 as a function of emission angle. Vertical scale is arbitrary. For $j=3$ the first maximum occurs at 9.8° and the first minimum occurs at 16.2°. For the fifth harmonic the values are 7.6° and 12.6°, respectively. Fundamental frequency is 2.85 GHz. Electron-beam parameters and index of refraction are as described in the text. Emitted power per unit solid angle is equal to a constant multiplying D_j as stated in (8).

Each harmonic is displaced differently, with the lower one displaced further from $\theta_{\check{C}}$. (Earlier, the radiated power was evaluated assuming the $\sin^2\theta$ factor to be constant; but even in that approximation it was noted that higher harmonics would be spread less from $\theta_{\check{C}}$.)

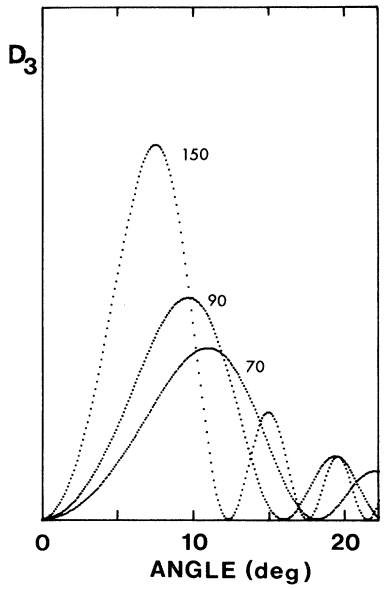

FIG. 5. Third-harmonic radiation function $D_3(\theta)$ as a function of emission angle for gas- (air-) cell lengths of 70, 90, and 150 cm. Vertical scale is arbitrary, and the same for all three curves. The peaks occur at 11.1°, 9.8°, and 7.6°, respectively. Electron beam parameters as given in the text.

Further consideration of Fig. 4 also suggests the large amount of total power radiated into larger angles, this effect being enhanced by an additional $\sin\theta$ factor (from the solid angle) which multiplies (9) in the expression for total power. To illustrate, also, that the spreading of intensity about the Čerenkov angle is an interference effect associated with the finite gas-cell length, $D_j(\theta)$ is calculated for several cell lengths, 70, 90, and 150 cm (usually 90 cm is assumed elsewhere in this paper), for the harmonic $j=3$ in Fig. 5. For longer cells, the peak in the main lobe moves toward $\theta_{\check{C}}$ but the approach is very slow. However, it is understood rather easily. The first null occurs when the Huygens waves emitted from the front and rear of the cell (of length L) differ in phase by 2π, which gives simply the condition obtained by setting $u=\pi$ in (11):

$$kL(\cos\theta_{\check{C}}-\cos\theta)=2\pi\ . \tag{12}$$

Then the reason for the large breadth of the lobe is that for the assumed condition, $\cos\theta$ varies slowly so that a large change in θ is required for the 2π phase shift required by (12) for a null.

To show what might be observed in an experiment, Fig. 6 displays the sum of $D_j(\theta)$ for harmonics $j=3,4,5$ and shows the expected washing out of diffraction zeros which occur at different emission angles for different harmonics. These harmonics would be seen by an X-band detector, with sensitivity from 8 to 12 GHz, assuming $\nu_0=2.85$ GHz for an S-band linac. The effect of adding the three radiation functions is to enhance and shift the first lobe and to smear out the interference effects at higher angles since the individual nulls in the D_j occur at different angles.

As the product kL increases, the position of the maximum in the radiation pattern decreases slowly to approach the Čerenkov angle. This behavior is shown in Fig. 7 where L is increased keeping the frequency (and thus k) fixed at the value for the third harmonic. The approach to $\theta_{\check{C}}$ is smooth, but significant differences are to be expected even at very long path lengths of 100 m.

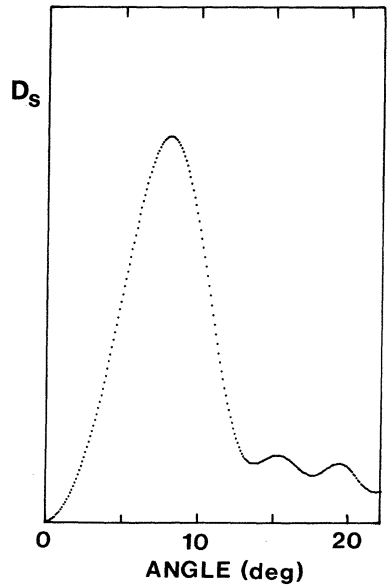

FIG. 6. D_s, the sum of $D_j(\theta)$ for $j=3,4,5$, as a function of θ. Electron-beam parameters and index of refraction are as described in the text. Emitted power per unit solid angle is equal to a constant times D_s. The maximum in D_s occurs at $\theta=8.30°$.

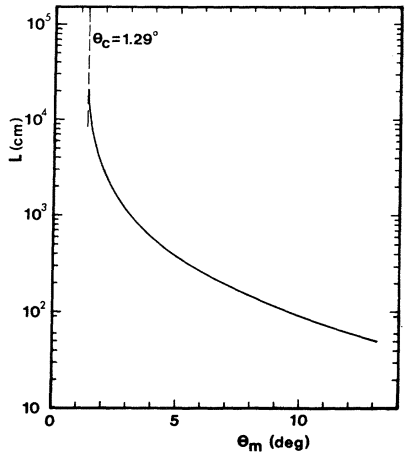

FIG. 7. Dependence of the first maximum in $D_3(\theta)$ as a function of gas (air) path length.

POWER RADIATED

In the earlier sections it was shown that power is radiated in a range about the Čerenkov angle, as is shown in Figs. 4 and 5. It is interesting to compare the total power radiated with the predictions of the approximation used in the earlier paper. In Fig. 8, two measures of power radiat-

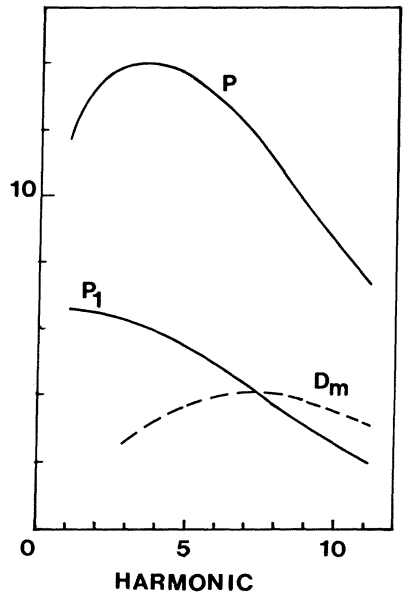

FIG. 8. Radiated power as a function of linac harmonic number. P is the total radiated power obtained by integrating D_j from 0 to π. P_1 is the radiated power in the first lobe of the radiation pattern. D_m is the maximum value of D_j, i.e., the value of D_j at D_m. All calculations are for $L=90$ cm and other parameters as given in the text. Vertical scale is in cm^2. Actual powers can be obtained by multiplying by $2\pi Q$.

TABLE II. Total radiated power as determined by numerical integration and by the approximation of Ref. 4. Power in the first lobe of the radiation pattern is also included. Parameters are as described in the text. Units are arbitrary.

Harmonic (n)	A Total power (numerical integration)	B Power in first lobe (numerical integration)	C Total power (approximation)	A/C
1	11.86	6.65	0.1174	101.02
2	13.53	6.59	0.228	59.34
3	14.12	6.34	0.324	43.58
4	14.12	5.96	0.402	35.12
5	13.71	5.49	0.459	29.87
6	13.52	5.01	0.491	27.54
7	12.06	4.37	0.512	23.55
8	10.99	3.78	0.492	22.34
9	9.86	3.20	0.464	21.25
10	8.72	2.66	0.425	20.52

ed are plotted as functions of frequency: (a) the total power and (b) the power integrated over the main diffraction lobe. Also shown is the peak power per unit solid angle in the main lobe. These display a rise at low frequency characteristic of Čerenkov radiation, followed by a fall-off at high frequencies, associated with the form factor of the bunch. The total power has a shape similar to that merely sketched in Ref. 4. The peaks in (a) and (b) occur at different frequencies and the approximate expression (6) [Eq. (32) of Ref. 4] would peak at still a different frequency.

A most surprising result is obtained when the total power and the power in the main lobe are compared to the approximate value. These results are given in Table II; additionally, the ratio of the total power to that predicted by the approximation is tabulated in the last column. This ratio has values of about 50 for the lower harmonics and gradually falls off at the higher frequencies. Noting from Fig. 8 that the power spectrum peaks at about the third or fourth harmonic, the above ratio has values from 35 to 43, meaning that the total Čerenkov radiation per unit length, under assumed conditions, would be larger by a factor of about 30 compared to what is expected from an infinite gas cell.

The physical reason for this large increase in the power radiated from a finite cell or path length may be illuminated by examining (4). The factor $F(\vec{k})=\tilde{\rho}'_0(\vec{k})/q$ describes the distribution of charge in the bunch and merely allows coherence at low frequencies, but partial cancellation as the wavelength of emitted radiation approaches the bunch length, and does not contribute to the power increase. This effect is governed by the two factors $\sin^2\theta$ and $I^2(u)$; the latter, through its argument u, governs phase matching of the electron and the emitted wave from the beginning to the end of the gas cell (of length L). Perfect phase matching occurs for $u=0$ or $\cos\theta=\cos\theta_{\check{C}}=c/v$. But for a finite cell, perfect phase matching is not required; as θ changes from $\theta_{\check{C}}$, the radiation from the various parts of the cell tends to cancel. In particular, a null should occur when the radiation from the front and rear elements are out of phase by 2π. This phase difference of 2π is obtained at an angle θ_N for which $kL=2\pi$, and therefore $I(u)=0$. The fact that u contains $\cos\theta$, and θ is near zero for a gas, results in a relatively broad peak. This breadth, combined with the $\sin^2\theta$ factor in the intensity, results in the large intensity emitted at angles larger than $\theta_{\check{C}}$, between $\theta_{\check{C}}$ and the angle for the first null θ_N. Also, the $\sin^2\theta$ factor accomplishes the increase in power, even if $\theta_{\check{C}}$ is small enough so that the null for θ less than $\theta_{\check{C}}$ (i.e., $u=-\pi$) is out of the physical range $\cos\theta\leq 1$.

CONCLUSIONS

The object of this paper is to consider in more detail the phenomenon predicted earlier, that the Čerenkov radiation, in cases where the interaction region is finite, should be broadened about the Čerenkov cone. For the case of a gas, for which the ordinary Čerenkov angle is a few degrees, the broadening is asymmetric about the Čerenkov cone, and the radiated power displays various interference lobes. The calculations and experiments are in agreement as to the position of the main Čerenkov radiation peak. For the X band, the position of the calculated peak as shown in Fig. 6 (8.30°) is very close to the peak angle (8.25°) shown in Table I which was derived from the measurements shown in Figs. 2 and 3. As the frequency of the Čerenkov radiation increases the peak angle decreases as shown in Fig. 4 for the third and fifth harmonics of the radiation, and this conclusion is supported by the K-band results also listed in Table II.

Considerable power (about half in the case of a gas) appears outside the main lobe, and the latter is peaked at angles much larger than the Čerenkov angle. An even more interesting result is that the Čerenkov power radiated per unit path length is increased by large factors approaching 2 orders of magnitude for a gas path of finite length compared to one of infinite length.

This increase in power is associated with the finite length of the radiating medium only. The effect should be approximately the same for either single or periodic electron bunches and should occur whether the bunches

are effectively point charges or have significant size.

To recall results obtained earlier, periodic bunches produce Čerenkov radiation at harmonics of the bunch frequency, while a single bunch will radiate with a continuous frequency distribution. The effect of the bunch size is reflected in the factor of the Fourier transform of the charge in the bunch, which causes the radiation to fall off at high frequencies, while at low frequencies all charges in the bunch radiate in phase.

The results outlined previously might occur in other situations or applications. The distinct phenomena are (a) coherent radiation by an electron bunch for wavelengths larger than the bunch, (b) radiation at harmonics of the bunch frequency, (c) smearing of the Čerenkov angle, and (d) asymmetric smearing of the Čerenkov angle with an increase in the power radiated. (c) and (d) should occur for finite radiator length; (d) should occur only if $\theta_{\check{C}}$ is very small.

All of the above are easily realized in the microwave region, where appropriate bunching occurs for traveling-wave accelerators. Possibly useful submillimeter wavelength radiation could be realized.

In the optical range, (c) and (d) could occur for radiating cells which could be as large as 100 μm in length. (a)—(d) together could only be realized with the small-scale bunching that occurs in a free-electron laser.[7]

For the X-ray region it is impossible to envision bunching fine enough to accomplish (a) and (b). The dielectric constant is less than unity, so that Čerenkov radiation does not generally occur. It might be possible to accomplish (c) and (d) if small spectral regions could be found in a medium for which the Čerenkov condition is satisfied, such as near an atomic resonance.[6] Then greatly enhanced radiation could be produced by using a thin layered structure for a medium.

ACKNOWLEDGMENTS

This work was partially supported by the U.S. Naval Postgraduate School Foundation Research Program and partially supported by the Office of Naval Research, U.S. Department of the Navy.

[1]V. P. Zrelov, *Čerenkov Radiation in High Energy Physics* (Israel Program for Scientific Translations, Jerusalem, 1970).

[2]T. Erber and H. C. Shih, Acta Phys. Austriaca XIX, 17 (1964).

[3]B. M. Bolotovskii, Usp. Fiz. Nauk 75, 295 (1961) [Sov. Phys.—Usp. 4, 781 (1962)].

[4]F. R. Buskirk and J. R. Neighbours, Phys. Rev. A 28, 1531 (1983).

[5]F. R. Buskirk and J. R. Neighbours, U.S. Naval Postgraduate School Report No. NPS-61-83-003 1982 (unpublished).

[6]V. A. Bazylev, V. I. Glebov, E. I. Denisov, N. K. Zhevago, M. A. Kumakhov, A. S. Khlebnikov, and V. G. Tsinoev, Zh. Eksp. Teor. Fiz. 81, 1644 (1981) [Sov. Phys.—JETP 54, 884 (1981)].

[7]A. P. Kobzev and I. M. Frank have noted that in the optical case the width of the Čerenkov cone depends on the radiator thickness. See A. P. Kobzev, Yad. Fiz. 27, 1256 (1978) [Sov. J. Nucl. Phys. 27, 664 (1978)]; A. P. Kobzev and I. M. Frank, *ibid.* 31, 1253 (1980) [31, 647 (1980)]; 34, 125 (1981) [34, 71 (1981)]. Equation 4 of the second reference above is similar to our formulation, except it refers to a point source radiator only.